

**Chemistry and Physics of
Rapidly Solidified Materials**

Edited by B.J. Berkowitz and R.O. Scattergood

CONFERENCE  PROCEEDINGS

The Metallurgical Society of AIME

Chemistry and Physics of Rapidly Solidified Materials

Proceedings of a symposium sponsored by the Chemistry and Physics of Metals Committee of The Metallurgical Society of AIME, the Corrosion and Environmental Effects Committee of The Metallurgical Society of AIME, and the Phase Transformation Activity of the American Society for Metals, held at the Fall Meeting of The Metallurgical Society of AIME, St. Louis, Missouri, October 26-27, 1982.

Edited by
B. J. Berkowitz
Exxon Research and Engineering
Florham Park, New Jersey
and
R. O. Scattergood
North Carolina State University
Raleigh, North Carolina

A Publication of



The Metallurgical Society of AIME

A Publication of The Metallurgical Society of AIME
420 Commonwealth Drive
Warrendale, Pennsylvania 15086
(412) 776-9000

The Metallurgical Society and American Institute of
Mining, Metallurgical, and Petroleum Engineers are
not responsible for statements or opinions in this publication.

© 1983 by American Institute of Mining, Metallurgical,
and Petroleum Engineers, Inc.
345 East 47th Street
New York, NY 10017

Printed in the United States of America.
Library of Congress Card Catalogue Number 83-061484
ISBN Number 0-89520-460-6



Foreword

The rapid solidification of materials leads to new and often unique non-equilibrium microstructures that can give rise to significant changes in properties. Because of the excellent potential for improved properties, there is a very active interest and ongoing research thrust in the area of rapidly solidified materials. Much of the initial work has been concerned with the technology for producing rapidly solidified powder, ribbon, or surface-modified bulk materials. In parallel with this, there has also been extensive, related work on the characterization of the non-equilibrium microstructures and the effect of processing variables on these structures. As with any emerging technology, the early focus tends to be on processing and characterization per se; however, as the technology matures, one can anticipate a greater emphasis on more-basic materials science aspects of the processing principles and the structure-property relationships. We believe that the area of rapidly solidified materials has reached the state of maturity where it is appropriate and timely to bring to the community at large the proceedings of a symposium aimed primarily at the fundamental aspects of rapidly solidified materials.

The symposium "Chemistry and Physics of Rapidly Solidified Materials" was held as part of the Fall Meeting of The Metallurgical Society of AIME in October, 1982, in St. Louis, Missouri. The symposium was sponsored jointly by the Chemistry and Physics of Metals Committee of TMS, the Corrosion and Environmental Effects Committee of TMS, and the Phase Transformation Activity of ASM. This volume contains the proceedings of that symposium. Emphasis was placed on thermodynamics, kinetics, and properties of rapidly solidified materials, as well as certain related areas of processing technology. Section I deals with thermodynamics and kinetics. The papers presented included investigations involving special experimental techniques as well as ones concerned with the development of new theoretical models. Section II contains papers on physical and chemical properties. These treat electronic, magnetic, corrosion, and mechanical properties. Section III contains pertinent papers on characterization and processing, which treat these topics from a fundamental viewpoint, and contain results that complement the earlier sections. The selection of papers in all sections include current research along with overviews on important subject matter.

We are grateful to the authors for their efforts and contributions to this symposium. We wish to thank The Metallurgical Society of AIME for supporting this symposium, and for making possible the publication of the proceedings.

The Organizing Committee

B.J. Berkowitz
Exxon Research and Engineering
Florham Park, New Jersey 07932

R.O. Scattergood
North Carolina State University
Raleigh, North Carolina 27607

Table of Contents

Foreword	v
--------------------	---

THERMODYNAMICS AND KINETICS

Rapid Solidification of Highly Undercooled Alloy Droplets <i>M.G. Chu, Y. Shiohara, and M.C. Flemings</i>	3
The Formation of Coarse Intermetallics in Rapidly Solidified Al-Co Alloys <i>R.K. Garrett, Jr. and T.H. Sanders, Jr.</i>	11
Structure Development in Melt-Spun Superalloy Ribbons <i>S.C. Huang and A.M. Ritter</i>	25
Production of Alternative Phases During Liquid-To-Solid Nucleation in Small Droplets <i>Thomas F. Kelly and John B. Vander Sande</i>	35
Solute Distribution in Highly-Supercooled Fe-25%Ni Alloy <i>D.D. McDavitt and G.J. Abbaschian</i>	49
Ostwald Ripening of Rapidly Solidified Solid-Liquid Mixtures <i>P.W. Voorhees and M.E. Glicksman</i>	63
Transformation Characteristics of Rapidly Solidified Shape-Memory Alloys <i>J.V. Wood</i>	79
Precipitation and Phase Stability in Some Rapidly Solidified Steels <i>J.V. Wood and J.V. Bee</i>	95

CHEMICAL AND PHYSICAL PROPERTIES

Amorphous Metal Coatings as Corrosion Barriers <i>R.A. Anderson, E.A. Dobisz, J.H. Perepezko, R.E. Thomas, and J.D. Wiley</i>	111
Accelerated Aging Behavior of an Iron Base Amorphous Alloy for 60 Hz Application <i>A. Datta, R.J. Martis, and S.K. Das</i>	127
Electronic Structure of Metallic Glasses <i>M.E. Eberhart, F.A. Leon, and K.H. Johnson</i>	139
Corrosion Resistance of Rapidly Quenched Alloys <i>R.M. Latanision, A. Saito, R. Sandenbergh, and S.-X. Zhang</i>	153

Mechanical Properties of Rapidly Quenched Metals and Alloys	173
<i>J.C.M. Li</i>	
Corrosion of an Amorphous $\text{Ni}_{40}\text{Co}_{20}\text{Cr}_{12}\text{Mo}_6\text{Fe}_6\text{B}_{16}$ Alloy	197
<i>T.K.G. Namboodhiri</i>	
Rapidly Solidified Fe-Si Based Crystalline Ribbons	211
<i>N. Tsuya, K.I. Arai, and K. Ohmori</i>	

CHARACTERIZATION AND PROCESSING

AES and XPS Analysis of Corrosion Layers Formed on Amorphous FeCrNiPB	221
<i>D.B. Baer and M.T. Thomas</i>	
Laser Glazing of $\text{Ni}_{60}\text{Nb}_{40}$	235
<i>R. Becker, G. Sepold, and P.L. Ryder</i>	
A Comprehensive Model of a Plasma Spraying Process	243
<i>N. El-Kaddah, J. McKelliget, and J. Szekely</i>	
The Effect of Neutron Irradiation on the Titanium Carbide Distribution in Rapidly Solidified Austenitic Stainless Steels of Varying Titanium and Carbon Content	261
<i>D. Imeson, C.H. Tong, J.B. Vander Sande, and O.K. Harling</i>	
Fe-B Glasses Formed by Picosecond Pulsed Laser Quenching	273
<i>Chien-Jung Lin and Frans Spaepen</i>	
The Characterization of Metastable Fe-Cr-C and Fe-C Metal Powders Produced Directly from the Mineral Concentrate Using Novel Plasma Reduction Technology	281
<i>J.J. Moore, P.J. Ryan, and J.M. Sivertsen</i>	
High Spatial Resolution Compositional Analysis in Rapidly Solidified Alloys	299
<i>John B. Vander Sande and Thomas F. Kelly</i>	
Subject Index	311
Author Index	315

Thermodynamics and Kinetics

RAPID SOLIDIFICATION OF HIGHLY UNDERCOOLED ALLOY DROPLETS

M.G. Chu Y. Shiohara M.C. Flemings

Materials Processing Center
Massachusetts Institute of Technology
Cambridge, Massachusetts
USA

Abstract

Experimental work is described on undercooling and structure of tin-lead droplets emulsified in oil. The droplets, predominantly in the size range of 10-20 μ m, were cooled at rates ranging from about 0.04 $^{\circ}$ K/sec to 10^6 $^{\circ}$ K/sec. The higher cooling rates were obtained by a newly developed technique of quenching the emulsified droplets in a cold liquid. Measured undercoolings (at the lower cooling rates) ranged up to about 100 $^{\circ}$ C. Structures obtained depended strongly on undercooling, cooling rate before nucleation, droplet size, alloy composition and the rate of heat extraction after nucleation.

Introduction

As the solidification rate increases, the dendrite arm spacing is reduced, supersaturation of the primary phase can occur, and metastable phases including metallic glasses can be formed. In each case, the liquid before nucleation or in front of the growing solid front must be substantially undercooled.

Controlled studies of highly undercooled metals and alloys (as in liquid emulsifications) are directly applicable to understanding rapid solidification. Moreover, it appears possible that new practical techniques for high undercooling and rapid solidification might be developed based on liquid emulsification, i.e., atomization in a liquid rather than in a gas or vacuum.

In this work, high undercooling was generated by the emulsification method developed by Perepezko and his co-workers. Emphasis is on the microstructures of solidified Sn-Pb alloy droplets with high undercoolings, cooled at different rates.

Experimental

The preparation of emulsified tin-lead droplets has been described else

where(1). In the case of experiments conducted at relatively low cooling rates, the emulsions were next transferred to sealed aluminum pans and placed within the DSC. The samples in these experiments typically consisted of 2mg of alloy droplets and 15ml oil. They were heated and cooled in the DSC at rates of 2.5, 5, 10, 20, 40, and 80 °C/min.

To cool the droplets more rapidly, the rapid quenching apparatus illustrated in Figure 1 was developed. Samples of emulsified tin-lead alloy were first placed within a heated shock tube. The samples were then reheated until the metal droplets were molten and then ejected into a uniformly agitated, cool fluid. The fluid used was a solution of CCl₄ in oil, held at several temperatures (50, 25, -4, and -25 °C). The emulsified metal was rapidly discharged into the stirred cold fluid by gas pressure entering through the valve shown. The emulsification was typically at 50 °C above its liquidus when ejected. Emulsifications used in these latter experiments were usually those for which undercoolings had previously been measured in the DSC. Actual undercoolings obtained at the more rapid rates were presumably higher.

Result

Undercooling Measurements. Undercoolings achieved depended to a considerable extent on the initial composition of the liquid. Figure 2 shows typical DSC results for different initial compositions at 10 °C/min heating and cooling rates. The thermal heating curve shows two endothermic peaks due to melting. The first peak indicates the melting of eutectic phase. The second peak corresponds to the melting of the primary tin or lead-rich phase. During cooling, one nucleation temperature was recorded for compositions containing less than 20wt%Pb. For compositions containing more than 25wt%Pb, two nucleation temperatures were recorded. The shaded area in the figure related to the latent heat of fusion for the alloy emulsions.

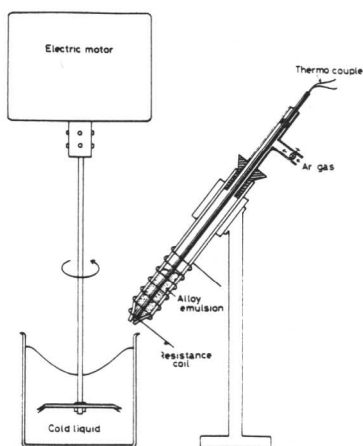


Fig. 1. Schematic diagram of the experimental apparatus for rapid quenching emulsified droplets.

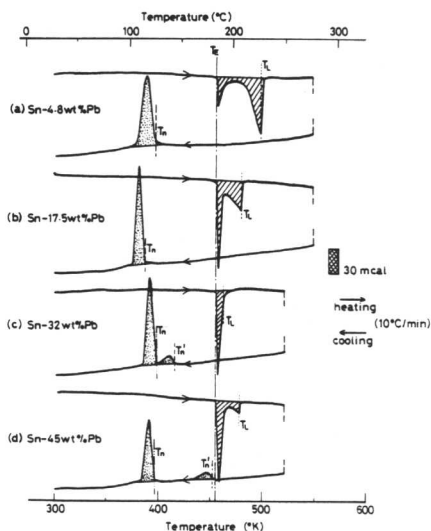


Fig. 2. DSC thermograms of four different Sn-Pb alloys.

These nucleation temperatures are plotted on the phase diagram of Figure 3. The surface coating on each droplet in this experiment was produced by air oxidation. Results obtained are in good agreement with results obtained by Perepezko et al. (2) for similarly prepared samples. The oxide film acts as a strong heterogeneous catalyst for the lead rich primary phase, so even in the case of hypo-eutectic compositions above 20wt%Pb, the lead-rich phase nucleates first. Only at the T_n temperature does the tin-rich phase nucleate grow. For compositions less than 20wt%Pb, the nucleation temperatures are almost parallel to the liquidus line; the phase nucleating is the tin-rich primary phase.

The phases forming at T_n and T'_n at different compositions were deduced in several ways. One way was by interrupted thermal cycles for 45wt%Pb alloy emulsion (Fig. 4). After remelting the emulsion, it was cooled at 10 °C/min cooling rate to the temperature below the first nucleation temperature and then reheated again at 10 °C/min. This heating curve shows only one peak due to melting of primary phase. This result indicates that at T'_n temperature, the primary lead-rich phase nucleates and solidifies and at T_n temperature, the tin-rich phase nucleates and solidifies. A second method of determining the phases that form at different temperatures is by the structural studies described later in this paper.

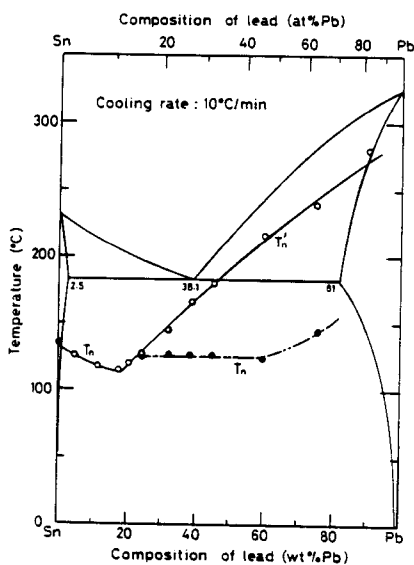


Fig. 3. Composition dependence of nucleation temperatures for Sn-Pb alloy droplets observed in DSC measurement with 10 °C/min cooling rate.

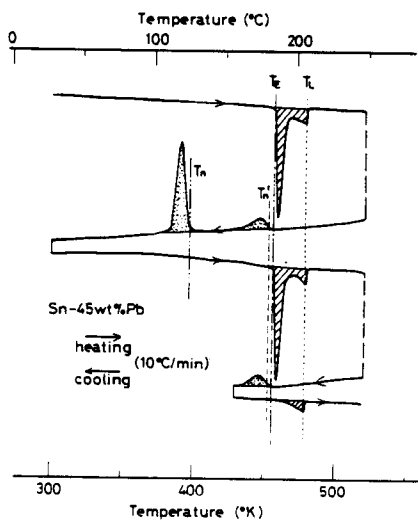


Fig. 4. DSC thermogram for Sn-45wt%Pb. On thermal cycling, when the sample is heated from room temperature, a peak is seen at T_E indicating presence of two phase. When the sample is heated from above T'_n but below T_n , a peak is observed only well above T_E , indicating only one solid phase formed at the nucleation temperature T_n .

The effect on undercooling of cooling rate before nucleation could be measured in the DSC at relatively low cooling rates (Figure 5). As the cooling rate increased within this range, the amount of undercooling did as well. The increase of undercooling is in a stronger function than that predicted by J.P. Hirth (3). This result suggests that at very rapid quenching rates of this emulsion such as these, quite high undercoolings might be obtained.

Microstructure Studies

Figure 6 shows the cross-sectional microstructures of droplets taken by a SEM (Scanning Electron Microscope). The droplets shown are from samples used after DSC measurements at 10 °C/min cooling rate to room temperature (Fig. 3). In these pictures, the dark gray phase is tin-rich, the white phase is lead-rich.

Samples below 20wt%Pb show a tin-rich matrix with a lead rich phase distributed uniformly. Samples from 20wt%Pb to almost 45wt%Pb show a light, lead-rich two phase region surrounded by a darker tin-rich two phase region. Samples containing larger amounts of Pb show again a largely uniform two phase structure, this time with a lead-rich matrix.

Figure 7 shows the cross-sectional microstructures of the droplets (Sn-25wt%Pb) which were cooled at the different cooling rate before nucleation (5, 10, 20, 40, and 80 °C/min). These cooling rates were automatically controlled to the room temperature in the DSC. The fraction of the primary Pb rich phase decreases with increasing the cooling rate. The small lead-rich second phase in the large tin-rich phase becomes finer with increasing the cooling rate.

When these same Sn-25wt%Pb droplets were rapidly solidified in cold liquid (using the apparatus of Figure 1), very different microstructures were obtained, Fig. 8.

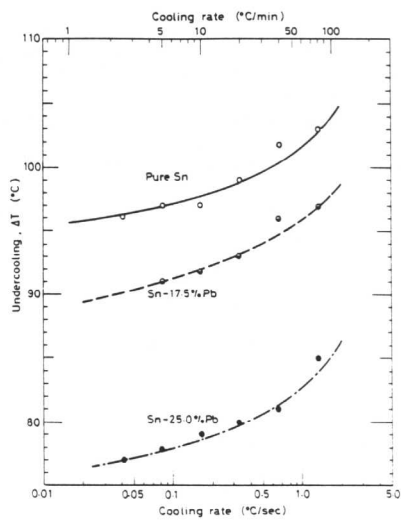


Fig. 5. Effect of cooling rate in the DSC on undercooling of pure Sn and two Sn-Pb alloys.

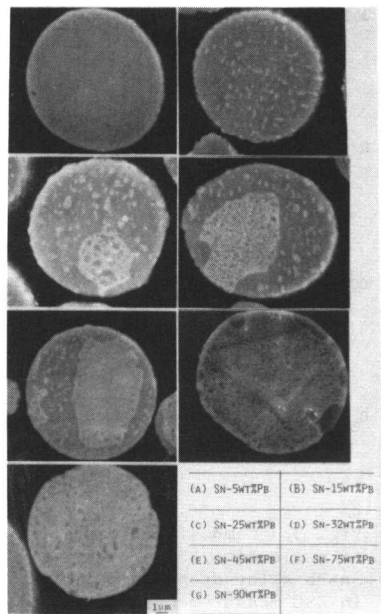


Fig. 6. Microstructures of droplet of seven Sn-Pb alloys solidified in the DSC at 10 °C/min.

There is no lead-rich two phase region; the structure consists of small lead-rich precipitates uniformly distributed in a Sn-rich matrix, much like low wt%Pb alloys solidified at lower cooling rates. Perepezko has obtained a similar structure in the eutectic alloy composition at low cooling rates by achieving higher undercooling at these low cooling rates than those usually obtained in this work.

A series of experiments were next done on Sn-5wt%Pb alloy quenched into a medium whose temperature was varied from +50 °C to -25 °C. Lowering the temperature of the quench medium resulted in a finer distribution of the lead-rich phase, and always, less of it, Fig. 9. When, finally, the Sn-5wt%Pb was quenched in fluid at -25 °C and special precautions were taken to keep the particle below room temperature until metallography was performed, a "featureless" microstructure was obtained when examined at 1000X, Fig. 10. After an extended period at room temperature, however, significant lead-rich phase precipitates from the supersaturated Sn matrix, Fig. 11.

The development of the morphology of the two-phase regions in samples of higher composition solidified at low cooling rates was elucidated with a series of experiments on Sn-45wt%Pb alloy. When rapidly cooled, (by quenching into the CCl₄/oil (½) bath at 25 °C), the resulting structure was fine dendritic, Fig. 12a. Next, droplets of the alloy were slowly cooled to just before the first nucleation temperature, T_n, and rapidly quenched. The resulting structure, Fig. 12b was similar, but somewhat coarser. Lastly, when the alloy was slowly cooled (10 °C per minute) through complete solidification, the light lead rich phase coarsened into the agglomerate structure in Fig. 12c (similar to the one in Fig. 6e).

Discussion

Much more work must be done to provide a complete and quantitative description of solidification of undercooled alloy such as Sn-Pb alloys

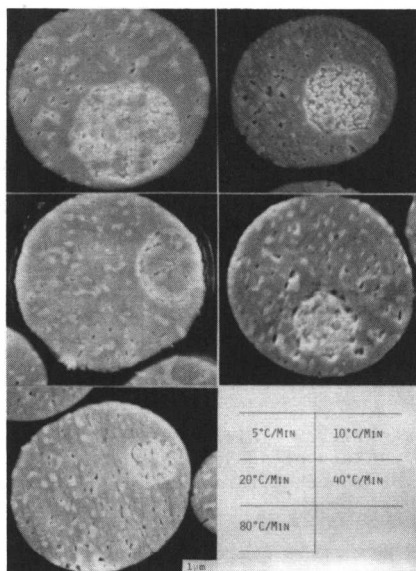


Fig. 7. Microstructures of droplets of Sn-25wt%Pb alloy solidified in the DSC cooling rate of 5-80 °C/min.

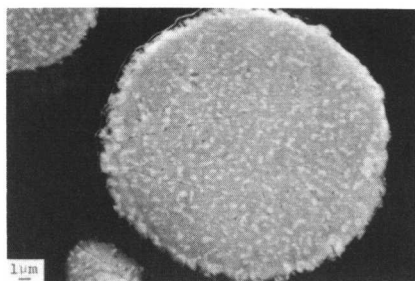


Fig. 8. Microstructures of droplets of Sn-29wt%Pb alloy solidified by rapid quenching in a solution of CCl₄ and oil at -30 °C.

discussed herein. However, structures obtained in this work are compatible with the quantitative description of solidification behavior given below; analytic work is now in progress and will be described in latter paper.

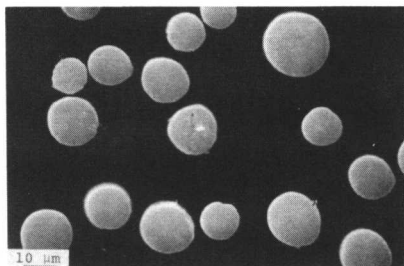


Fig. 9. Microstructures of droplets of Sn-5wt%Pb alloy rapidly quenched in a bath at -25°C .

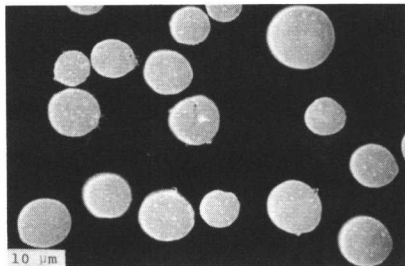
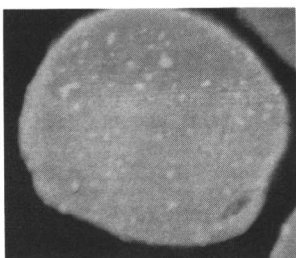
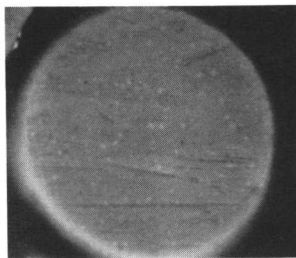


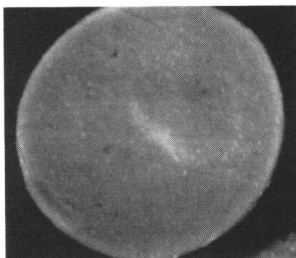
Fig. 10. The same droplets shown in Fig. 9, after one month at room temperature, note the substantial precipitation of lead-rich phase.



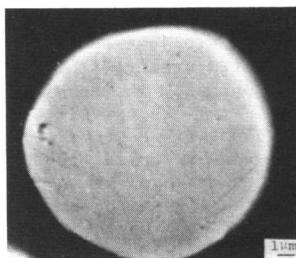
a



b



c



d

Fig. 11. Microstructures of droplets of Sn-5wt%Pb alloy superheated 50°C and rapidly quenched in bath at temperature: (a) 50°C (b) 25°C (c) -4°C (d) -25°C .

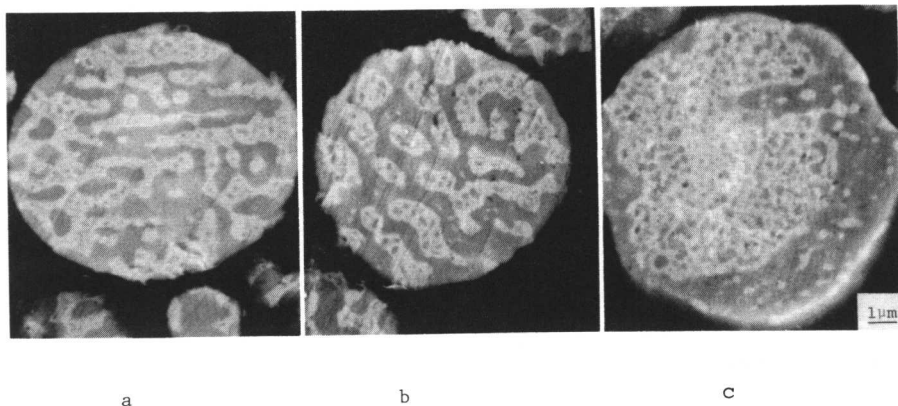


Fig. 12. Microstructures of Sn-45wt%Pb alloy droplets.
(a) Rapidly quenched (b) Slowly cooled to just below T_n
and quenched (c) Slowly cooled to room temperature.

When droplets with compositions less than about 20wt%Pb cool to the nucleation temperature (T_n , Fig. 3), nucleate, and supersaturated Sn-rich thermal dendrites then grow in a "diffusionless" fashion until the " T_0 " temperature is reached, where liquid and solid free energies are equal.

As recalescence continues above T_0 , solidification can no longer be partitionless, and local pockets of Pb-rich interdendritic liquid must then develop. Eventually, a maximum recalescence temperature, T_R , is reached, where heat generation from recalescence is balanced by local rate of heat extraction into the surrounding cooler emulsifying medium. Thereafter, cooling rate of the undercooled droplets becomes very high -- readily exceeding 10^5 °C/s even without supplemental quenching into a cold fluid. This high local rate of heat extraction results from heat flow from each droplet to the surrounding emulsifying medium which has cooled to the nucleation temperature T_n .

During cooling, solidification of the droplets continues at sufficiently low cooling rates and a second phase (Pb-rich) can form, although we have not yet observed this on the DSC. The second phase can also, of course, precipitate during subsequent cooling to room temperature or holding at room temperature.

Increasing the rate of heat extraction by increasing the cooling rate in the DSC, or by quenching the recalescing emulsification, reduces the time available for coarsening and would therefore be expected to reduce the size of second phase particles precipitating from the melt.

Alloys containing large amounts of Pb (e.g. Sn-90wt%Pb, Fig. 6g) appear to solidify much as described for Sn-rich alloys. The resulting structure has small Sn-rich particles uniformly distributed in a Pb rich matrix after the relatively slow solidification, and this is presumably largely if not completely from solid state precipitation.

At lower Pb contents, down to about 25wt% or so of Pb, we must distinguish between slow and fast rates of heat extraction to describe the genesis of the solidification structures observed. Consider first Sn-45 wt%Pb solidified at rapid rates of heat extraction (e.g. quenched in

CCl₄/oil bath). Pb rich dendrites form not greatly below T_n' and grow, first with some recalescence and then during cooling to T_n . At T_n , Sn-rich phase nucleates (with some recalescence), and subsequent solidification occurs as in alloys below about 20wt%Pb for Sn-rich alloys. The amount of Pb rich precipitate in the final Sn-rich part of the structure depends on rates of heat extraction (as does the amount of Sn-rich precipitate in the Pb-rich dendrites).

At slower rates of heat extraction, solidification of this Sn-45wt%Pb alloy occurs much as it does at more rapid rates, except the primary dendrite Pb-rich dendrites have much more time to ripen and agglomerate, as shown in Fig. 12c. There is also, of course, greater amounts of precipitation and coarser precipitates with the Sn and Pb rich phases.

Acknowledgement

The authors gratefully acknowledge support of this research by NASA contract NSG-7645.

References

1. Y. Shiohara, M.G. Chu, D.G. MacIsaac and M.C. Flemings, to be published in Proceedings of the Materials Research Society Annual Meeting, Nov. 1981, Boston.
2. K.P. Cooper, I.E. Anderson and J.H. Perepezko, Rapidly quenched metals IV, Vol. 1, edited by T. Masumoto and K. Suzuki, The Japan Institute of Metals, 107(1981).
3. J.P. Hirth, Metallurgical Transactions, Vol. 9A, 401(1978).

THE FORMATION OF COARSE INTERMETALLICS IN

RAPIDLY SOLIDIFIED Al-Co ALLOYS

R. K. Garrett, Jr., T. H. Sanders, Jr.

School of Materials Engineering
Purdue University
West Lafayette, IN 47907
USA

This paper presents a phenomenological mechanism to describe the morphology of intermetallic phases in rapidly solidified Aluminum-Cobalt alloys.